Chemical Engineering Journal 158 (2010) 345–352

Contents lists available at ScienceDirect

Chemical Engineering Journal

journal homepage: www.elsevier.com/locate/cej

Photocatalytic study of two-dimensional ZnO nanopellets in the decomposition of methylene blue

W.S. Chiu [a,*], P.S. Khiew [a], M. Cloke [a], D. Isa [a], T.K. Tan [a], S. Radiman [b], R. Abd-Shukor [b], M.A. Abd. Hamid [b], N.M. Huang [c], H.N. Lim [d], C.H. Chia [c]

[a] Department of Chemical Engineering, Faculty of Engineering, University of Nottingham Malaysia Campus, Jln Broga, 43500 Semenyih, Selangor Darul Ehsan, Malaysia
[b] School of Applied Physics, Faculty of Science & Technology (UKM), Universiti Kebangsaan Malaysia, 43600 Bangi, Selangor Darul Ehsan, Malaysia
[c] Department of Physics, Faculty of Science, University of Malaya, 50603 Kuala Lumpur, Malaysia
[d] Chemistry Department, Faculty of Science, Universiti Putra Malaysia, 43400 UPM Serdang, Selangor Darul Ehsan, Malaysia

ARTICLE INFO

Article history:
Received 7 September 2009
Received in revised form 22 January 2010
Accepted 25 January 2010

Keywords:
Zinc oxide
Two-dimensional nanopellets
Characterization
Photocatalyst
Methylene blue
Pseudo-first-order

ABSTRACT

We report several significant photodecomposition rates of methylene blue (MB) obtained before and after the refluxing process of own-synthesized two-dimensional (2D) zinc oxide (ZnO) nanopellets. Each photodecomposition rate of MB was found highly dependent on the weight of photocatalyst. The existing photodecomposition rate has been successfully improved to a factor of 22.0 times through refluxing process in excessive pyridine where the surface capping ligand (oleic acid) is removed from the 2D ZnO nanopellets. On the other hand, the refluxed photocatalyst (0.04 g) in this study was found to exhibit excellent recyclability up to three cycles. Furthermore, X-ray powder diffraction spectrums for the refluxed photocatatalyst, respectively, before and after three cycles of photocatalytic reactions, has generated the same patterns showing that the photocatalyst is stable and feasible to be used as an efficient photocatalyst material. Hence, these 2D ZnO nanopellets would provide a new alternative route as a highly efficient photocatalyst for wastewater treatment.

1. Introduction

Recently, quality drinking water has become a major concern worldwide due to the ever-increasing population and decreasing energy resources. Due to this reason, the efficient treatment of wastewaters have become immediate importance among science communities around the globe as there is a growing need to come out with the state-of-the-art technologies that are capable to solve the problems. Ideally, an effective wastewater treatment is to mineralize completely all the toxic contaminants in wastewater without leaving any hazardous residues. In addition, the wastewater treatment process should be cost-effective and feasible for large-scale applications.

Unfortunately, by the time being, only a limited number of employed treatment technologies such as activated carbon and biological methods, which somehow fulfilled the requirements mentioned above but there are still feeble aspects to be considered. Thus, it is necessary to find an alternative solution, which may offer a prominent route in industrial wastewater treatment process. Recently, nanotechnology has been widely adopted as an efficient way in dealing with clean water issues. In conjunction with the applications of nanomaterials in wastewater treatment, the utilization of semiconductor nanomaterials as an effective photocatalyst in wastewater treatment had been drawn much attention among scientific communities.

Recent advances in colloidal synthesis enable the precise design of high performance photocatalyst in terms of activity, selectivity and resistance to deactivation. Various advanced-synthetic techniques have been pursued in designing congruent photocatalyst materials for the decomposition of organic dyes [1–3]. The understanding of the properties, which may affect catalytic performance, is of great importance. However, not all the semiconductor materials are suitable to be used as efficient photocatalysts due to their stabilities against oxidation. For example, the well-known CdSe semiconductor nanocrystals have been widely used in bio-labeling [4–6] as well as optoelectronic devices [7,8]. Nonetheless, the application of CdSe nanocrystals as photocatalyst is strictly hampered due to its stability against photo-oxidation. Hereby, its application as photocatalyst materials has remained a query since the formation of amorphous oxide layer was observed under ambient condition [9]. Thus, the idea of oxide-based semiconductors to be used as photocatalysts have been introduced thereafter to disclose the ideal photocatalyst characteristics like good photo- and thermal-stability, high selectivity, and excellent recyclability.

* Corresponding author. Tel.: +60 193292772; fax: +60 389248017.
E-mail address: WEE-SIONG.CHIU@nottingham.edu.my (W.S. Chiu).

1385-8947/$ – see front matter © 2010 Elsevier B.V. All rights reserved.
doi:10.1016/j.cej.2010.01.052

In accordance to the oxide-based semiconductor materials, there have been reports about the novelty in utilizing TiO_2 as a photocatalyst material. Utilization of this material for the decomposition of organic compounds has generated many promising results [10–12]. For last two decades, the demands of titanium worldwide have been raised due to various sophisticated mechanical application in aerospace, automobile fabrication, marine industry and novel biomaterials [13]. Due to the demanding importance of titanium in the industries mentioned above, the commercialization value for TiO_2 have steadily increased this few years and exceeding the value of ZnO [14]. Hence, alternative potential resources for titanium, which render the comparable efficiency, have to be considered. Among the oxide-based semiconductors that hold the promise as a potential photocatalyst, ZnO has reflected comparable efficiency to that of TiO_2. Analogous to TiO_2, ZnO could serve as an ideal photocatalyst candidate that is cost-effective and environment-friendly. Other than that, the comparable intrinsic bandgap energy of ZnO (3.37 eV) [15] to that of TiO_2 (3.2 eV) [16] also makes it (ZnO) a suitable candidate in absorbing UV-light as an excitation source. Recently, various reports have shown that ZnO are good photocatalyst materials. For instances, Sakthivel et al. found that ZnO nanoparticles exhibit higher rate than that of TiO_2 nanoparticles. They attributed this to the ability of ZnO in absorbing large fraction of the solar spectrum and more light quanta than that of TiO_2 [17]. Furthermore, Sun et al. have shown that photocatalytic rate and TOC removal efficiency of ZnO can be improved through modification of its morphology into dumbbell-shape [18].

For few decades, ZnO has been reported as a unique material that exhibits semiconducting, piezoelectric, and pyroelectric multiple properties [19]. Due to its unique intrinsic properties, which are relatively anisotropic, ZnO has been synthesized in various shapes and dimensions either it is in 1D, 2D or 3D. Additionally, many reports regarding the application of ZnO nanostructures especially in optoelectronic device have been logged [19–24]. However, most of these ZnO nanostructures are 1D ZnO. As a result, the intensive efforts put in the studies of 1D nanostructures have neglected the development of 2D ZnO nanostructures. Until now, there are limited reports on the application of 2D ZnO nanostructures especially as photocatalyst materials.

Hereby, for the first time we use own-synthesized 2D ZnO nanopellets in this study for the photodecomposition of MB. The as-synthesized 2D ZnO nanopellets are prepared via low-cost process using environment-friendly zinc oleate compound through simple one-pot pyrolysis reaction [1]. These nanopellets exhibit low photocatalyst rate due to the presence of oleic acid on its surface. However, we have successfully improved its (2D ZnO nanopellets with the weight of 0.04 g) photocatalytic rates to a factor of 22.0 times through refluxing process in excessive pyridine. There is no large variation in terms of both size and shape distributions after reflux. Hence, this treatment process may open a new route in the removal of capping ligand from nanomaterials surface and preserve its originality especially for nanomaterials prepared via organometallic approach.

Besides that, there are several other beneficial aspects of using 2D ZnO nanopellets as photocatalyst found in this study like the consistent efficiency, stability, ease of material synthesis, and advanced nanostructure of ZnO. Thus, in contrast to the study carried out by Formo et al. [25], the as-synthesized 2D ZnO nanopellets are more stable and exhibiting excellent recyclability up to three cycles, and no reactivation process is required to recover the loss of photocatalytic efficiency which is caused by poisoning effects. Moreover, the approaches used in photocatalytic reaction of ZnO, which are fixed-bed [26] and free-flow suspension, would as well influence the efficiency of photocatalysts. The free-flow suspension approach adopted in this study would provide more surface area of 2D ZnO nanopellets during photocatalytic process than that of fixed-bed and this would drastically contribute to higher photocatalytic rate. Furthermore, not only the solution synthesis of 2D ZnO nanopellets is producing higher yield if compared to that of gas phase synthesis, it is also a more economical route in industrial-scale wastewater treatment [27,28].

2. Experimental details

All the chemicals were used without further purification. Deionized water from Milli-Q-POD ultrapure water purification system (resistivity = 18.2 MΩ, TOC ≤ 5 ppb) was used throughout the experiment. MB trihydrate (Mallinckrodt, ≥99%) was selected as a model of organic dye for the evaluation of the photocatalytic activity. Details for 2D ZnO nanopellets preparation have been reported in previous study [1]. Pyridine (Merck, ≥99%) was used as solvent in removing excessive oleic acid that capped on the surface of 2D ZnO nanopellets. Anhydrous solvents including n-hexane (Aldrich, ≥99%) and ethanol (Aldrich, ≥99.5%) were used throughout the purification process after reflux.

The as-synthesized 2D ZnO nanopellets as reported [1] were refluxed for 8.0 h (at 60 °C under continuous purge of Ar gas with robust stirring) in pyridine to remove excessive oleic acid that capped on the surface of ZnO nanopellets. It was observed that some of the large-sized 2D ZnO nanopellets tend to form precipitate at the bottom of the flask after refluxing due to the successful removal of oleic acid from its surface. The sample was centrifuged to obtain the precipitation of 2D ZnO nanopellets in grayish form. The precipitation was subjected to disperse in anhydrous hexane and was precipitated by anhydrous ethanol with the assistance of centrifugation up to three times to remove the oleic acid that capped on the surface of 2D ZnO nanopellets initially. Finally, the precipitate was dried overnight in the oven.

Photodecomposition of 10.0 mL MB aqueous solution with an initial concentration of 5.00 ppm in the presence of various weights of 2D ZnO nanopellets were conducted in a heavy-duty Schott soda-lime test-tube (GL-18) under consistent UV irradiation. Prior to irradiation, the samples were sonicated for 2.0 min. Then, the samples were irradiated by using UV-crosslinker (UVP-CL1000, Cambridge), which is operating at a power of 8.0 W and equipped with high-pressure mercury lamp of 4.0 cm placed above the test-tube to provide irradiance wavelength of 254 nm. The average intensity of UV irradiance reaching the samples was measured to be ca. 100 $\mu J/cm^2$. Once the irradiation finished, the sample was centrifuged at 4000 rpm to separate the 2D ZnO nanopellets from the suspense. Micropipette was used to transfer the supernatant scrupulously into quartz cuvette (optical path length of 1 cm) to monitor MB concentration at wavelength of 665 nm (dominant peak for MB) by using UV–visible spectrophotometer.

The morphology of 2D ZnO nanopellets was characterized by transmission electron microscope (TEM) (Philips CM12 with operation voltage 100 kV). UV–visible spectrophotometer (Varian Cary 50 equipped with xenon flash lamp for best sensitivity and reduces excessive photometric noise filtration) was used for monitoring the absorption of MB. Nitrogen physisorption experiments were carried out using a Micromeritics ASAP-2020 analyser at −196 °C. Before the measurement, degassing was conducted at 200 °C for 2 h to remove possible moisture. X-ray diffraction (XRD) was used to identify the crystal structures using an X-ray diffractometer X'PERT PRO PW3040 (scanning rate 0.01°/s, Cu Kα radiation and wavelength, λ = 0.154 nm).

3. Results and discussion

Fig. 1 shows the TEM micrograph of the as-synthesized 2D ZnO nanopellets before and after refluxing process. The average

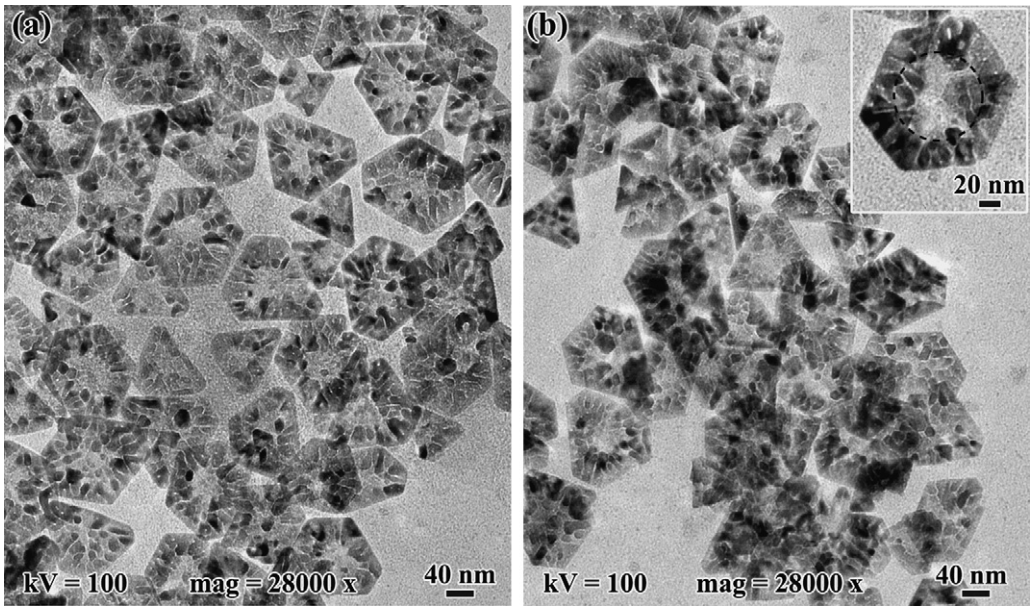

Fig. 1. TEM micrograph (magnification 28000×) of ZnO nanopellets annealed at 317 °C for 120 min (a) before refluxed (b) after refluxed in pyridine (inset: high-magnification (45000×) of selected 2D ZnO nanopellet with a hole at the center forming a ring structure).

edge length of the sample before reflux falls within the range of 40–125 nm and it has shown "shape distribution" both in triangular and hexagonal thin pellet form (Fig. 1(a)). On the other hand, the average edge length of the sample that has been refluxed for 8.0 h in pyridine does not show significant changes (Fig. 1(b)). The major difference is the increased tendency of agglomeration among nanopellets which would reduce overall surface energy as suggested by Yacaman et al. [29]. These nanopellets interact to each other via the weak Van der Waals force as an effect of lost steric repulsion that is resulted by the removal of oleic acid. However, these nanopellets can still be dispersed in water by carrying out a simple sonicating process.

In addition, there are no significant variations in morphologies for the samples that have been refluxed. As depicted in high-magnification TEM micrograph (inset in Fig. 1(b)), some of the nanopellets form a hole at the center caused by the continuous etching effect of oleic acid during synthesis. These morphologies are still preserved after reflux and they are believed to greatly benefit the photocatalytic reaction in providing more surface area which would increase the active reaction sites during heterogeneous catalysis reaction [30]. Various findings have shown that increasing numbers of surface atoms would greatly alter the electron density and subsequently change the ionization energies of photocatalysts. Hence, the rates of photocatalytic reaction could be enhanced by maneuvering the morphologies of photocatalysts to improve the electron transfer rates [31].

Fig. 2 shows the temporal changes in MB concentrations as the effects of photodecomposition initiated by various weights of 2D ZnO nanopellets after the samples were irradiated in UV-crosslinker for 6.0 h. After every interval of 1.0 h, the amount of MB left for each sample was simultaneously monitored by examining the various maxima absorptions at the wavelength of 665 nm by using UV–visible spectrophotometer. After irradiation, the intensities of the peaks shown in the spectrums decrease at this particular wavelength, which is due to the breaking of the conjugated π-system in MB chain [32]. Additionally, the diminished intensities of blue colour in MB solution (hypsochromic effect) were also observed. Prolonged times of irradiation cause the MB solutions to turn into pale white and finally these solutions become clear, and this phenomena implies that all or part of the auxochromic groups (methyl or methylamine) has degraded [33].

In the absence of any photocatalyst, (Fig. 2(a)), there is only slight decrease in the absorbance at maxima absorption even though it has been irradiated for 6.0 h. Thereby, obviously the photodecomposition process is very slow where only 17.83% of MB has undergone decomposition if it (photodecomposition process) merely depends on UV-light source without any photocatalyst. After addition of 0.04 g 2D ZnO nanopellets (without reflux in pyridine) (Fig. 2(b)), the photodecomposition of MB is greatly enhanced to 38.29% when irradiation is conducted for 6.0 h. The light-induced excitation process in charge donor semiconductor of ZnO has successfully triggered the photodecomposition process by creating adequate amount of electrophilic species that is necessary in initializing the degradation of MB.

Meanwhile, it was found that these 2D ZnO nanopellets were hardly dispersed in MB solution due to the oleic acid that bound on its surface despite the purification process was done for three times after synthesis process. Anyhow, this oleic acid plays an important role as capping ligand in inhibiting the agglomeration process and regulating the shape of nanocrystals during growth process [34]. Previous attempts including UV–ozone oxidation technique [35], plasma cleaning [36], hydrogen treatment [37] and heat treatment [38] have been employed for the removal of capping ligand. Unfortunately, not all treatment methods are suitable for removal of capping ligand from the surface of nanostructures because there are irreversible modifications of the shape and size distribution that would subsequently lead to interparticles agglomeration [38]. Hence, it is essential to find an alternative way in solving this matter for the benefit of nanomaterials preparation using colloidal method as colloidal chemistry is incorporating system-capping ligand in tailoring both the size and shape of the nanomaterials. Further study and utilization of these nanomaterials for various applications are strictly hampered due to the presence of capping ligand as impurities. Thus, it is very important to find a crucial and simple way to remove this capping ligand. As an effective method in removing capping ligand, it must be able to withdraw the capping ligand effectively without altering both the size and shape of the nanocrystals. Furthermore, it must be simple, feasible and cost-effective.

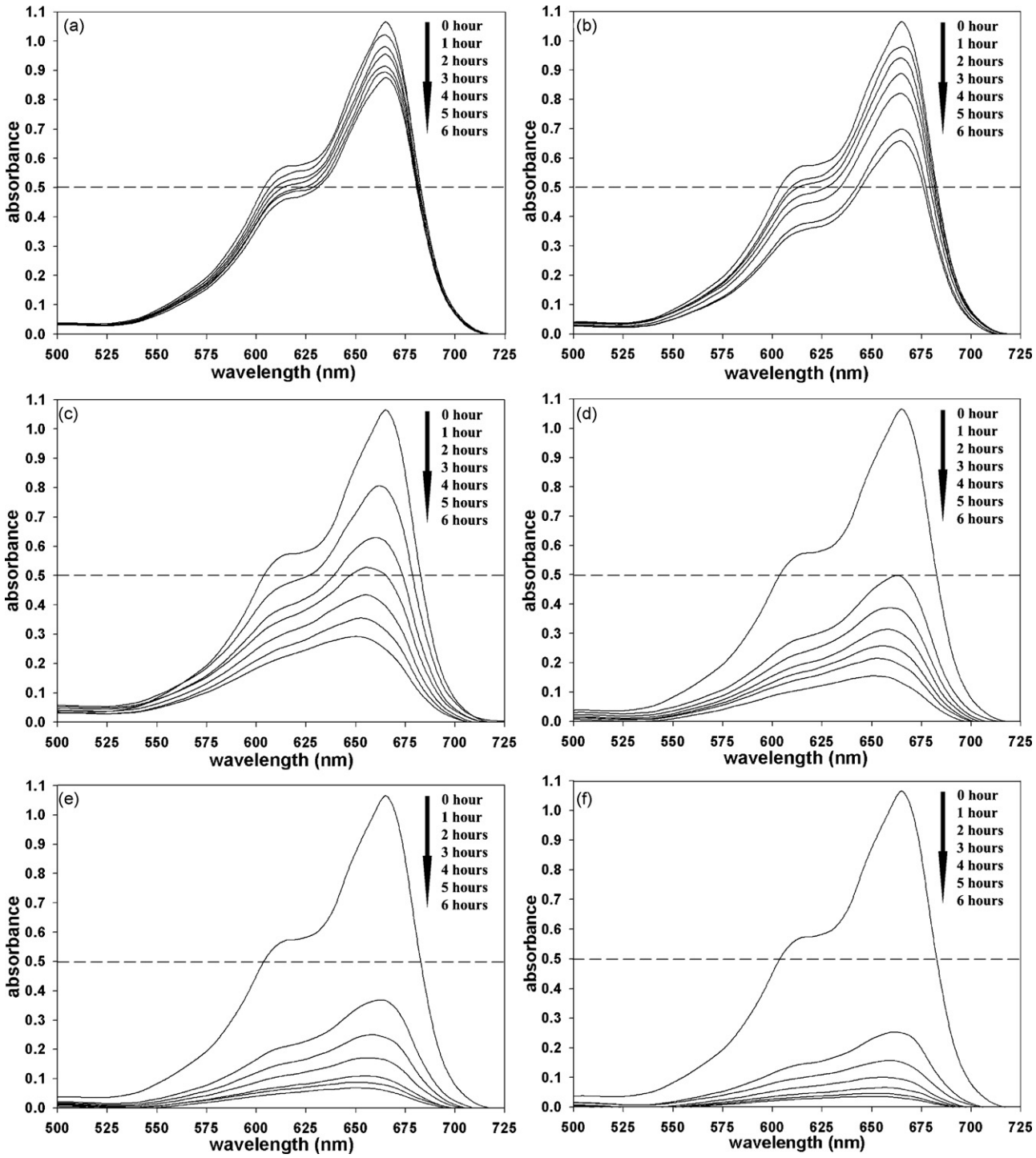

Fig. 2. Temporal changes in the concentration of MB monitored by examining the various maximal absorptions at the wavelength of 665 nm for: (a) MB without photocatalyst, (b) 0.04 g nanopellets before refluxed in pyridine, (c) 0.001 g nanopellets after refluxed in pyridine, (d) 0.005 g nanopellets after refluxed in pyridine, (e) 0.02 g nanopellets after refluxed in pyridine and (f) 0.04 g nanopellets after refluxed in pyridine (dash line indicating 50% decomposition of MB).

In current study, we have adapted the method reported by Sachleben et al. [39] to remove excessive oleic acid that binds on 2D ZnO nanopellets surface by refluxing the photocatalyst in pyridine at 60.0 °C for 8.0 h before photocatalytic test. According to Sachleben et al., they successfully used NMR technique to prove that pyridine can associate with CdS nanocrystal surface and rapidly exchanges on and off from the surface. In addition to that, Katari et al. also reported the successful result in using pyridine to displace trioctylphosphine oxide (TOPO), which is a very strong capping ligand that can anchor on CdSe nanocrystal surface [40]. Their XPS result shows that high purity CdSe nanocrystal can be obtained after evaporating off the pyridine molecules. On the other hand, it is generally understood that the high polarity of pyridine also makes it miscible with water and this enables the formation of stable suspension in water. Moreover, the exceedingly shorter hydrocarbon chain and lower steric barrier of pyridine compared to those of oleic acid also ease the accessibility of MB molecules to the surface of nanopellets.

Table 1 shows the surface area, pore volume and pore size analysis for the as-synthesized 2D ZnO nanopellets before and after refluxed. Before the ZnO nanopellets were subjected to reflux-

Table 1
Surface Area, pore volume and pore size analysis for 2D ZnO nanopellets before and after refluxed.

Sample	Surface area (m^2/g)	Pore volume (cm^3/g)	Pore size (nm)
ZnO nanopellets before refluxed	5.0921	1.0252×10^{-2}	10.4838
ZnO nanopellets after refluxed	9.0687	3.7154×10^{-2}	22.3342

ing process, the surface area was determined to be 5.0921 m^2/g. Meanwhile, the pore volume and pore size was found to be 1.0252×10^{-2} cm^3/g and 10.4838 nm, respectively. On the other hand, for the nanopellets that have been refluxed, the surface area increased to 9.0687 m^2/g. As a comparison, 68.89% of the surface area increment has been observed. Substantial variation in pore volume (3.7154×10^{-2} cm^3/g) and pore size (22.3342 nm) in accordance to the surface area changes have been observed as well. The increase of the surface area can be attributed to the efficient refluxing process that promotes the removal of oleic acid that capped on the nanopellets surface. During refluxing, an input energy has been supplied to oleic acid molecules to enable the expansion of its alkyl chain and subsequently promote its dissolution in the pyridine through reduction of its free energy. With prolong reflux process, the oleic acid molecules gain sufficient kinetic energy and finally diffuse away from nanopellets surface as free ligands.

The photodecomposition rate was successfully improved twice for MB with the presence of 0.001 g 2D ZnO nanopellets (Fig. 3(c)) if compared to the one without reflux (Fig. 3(b)). The amount of MB that decomposed was reported to be 76.65% after 6.0 h of UV irradiation. This implies that refluxing process is necessary in removing the oleic acid that occupied the catalytically active sites of 2D ZnO nanopellets. Hence, more MB can be absorbed on its surface without impedance caused by the oleic acid molecules and this would increase the efficiency of photodecomposition process. According to TEM micrograph (Fig. 1), most of these nanopellets are found to exhibit a shape of penetrable nanoring structure at its center, which is similar to that reported by Wang et al. [41] who used chemical vapor deposition (CVD) technique for the nanomaterials preparation. Besides that, a lot of bending contours were observed along the surface of the nanopellets structures. Therefore, these 2D ZnO nanopellets are less compact and could provide more active reaction sites for the absorption of MB after the removal of oleic acid.

As a comparison, the refluxed 2D ZnO nanopellets with various weights have been used for photocatalytic test. The photodecomposition rates were found to show dependency to the weight of photocatalyst, where higher doses of photocatalyst can greatly increase the photodecomposition rate. Having the weight of refluxed 2D ZnO nanopellets increased from 0.001 to 0.005 g, the amount of MB decomposed was improved to 87.69%. This value was increased to 94.49% when 0.02 g of nanopellets was used. Further increasing the weight of refluxed nanopellets to 0.04 g, it has successfully decomposed 97.16% of MB. This value was found to be 22.0 times faster than that of the one (nanopellets with identical weight) without refluxing process.

In addition to the removal of oleic acid that has contributed to the increase of photocatalytic rates, the unique nanofeatures provided by these 2D ZnO nanopellets are also believed to enhance the photocatalytic rates through improving the electron transfer rates [42–44]. This can be explained by the presence of contours that render the curvature textures along the surface of 2D ZnO nanopellets, which could better facilitate the physical absorption of MB than that of flat surface. These curvature textures would locally favor the absorption of MB during the reaction by forming a bidendate bonding, whereby MB is a compound that has a high tendency in forming monomer and dimmer in solution due to existence of the carbon–carbon double bond in the aromatic ring [45,46]. The different degrees of absorption on photocatalyst surface is one of the factors that govern the photocatalytic reaction rate as reported by Huang et al. who study the photodecomposition of rhodamine B and 4-chlorophenol by using ZnO nanowire [28].

Fig. 3 shows the efficiency comparison for various weights of 2D ZnO nanopellets as a function of irradiation times. For MB without photocatalyst (Fig. 3(a)), MB decomposed gradually and exhibited linearity with time. While in the presence of 2D ZnO nanopellets at different weights, the decompositions occurred with higher rates and the graphs deviated from linear to exponential decay (Fig. 3(b)–(f)). In order to elucidate the reaction rates, the data were re-plotted in $\ln(C_o/C)$ versus time (Fig. 4). As depicted in Fig. 4, all the photocatalytic reactions are almost approaching pseudo-first-order reaction. The respective rate constant, k was determined by calculating the slope of the graph in Fig. 4.

In accordance to the MB without any photocatalyst, the rate constant gave the k value of 0.0330 h^{-1} while this value increased to

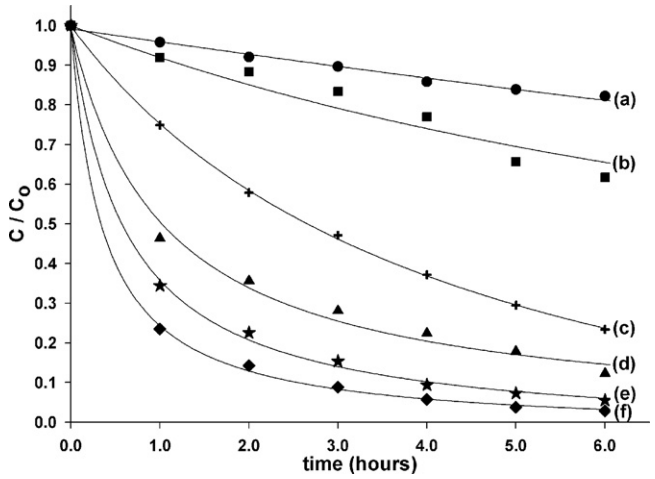

Fig. 3. Efficiency comparison of photocatalytic rate for: (a) MB without catalyst, (b) 0.04 g nanopellets before refluxed in pyridine, (c) 0.001 g nanopellets after refluxed in pyridine, (d) 0.005 g nanopellets after reflux in pyridine, (e) 0.02 g nanopellets after refluxed in pyridine and (f) 0.04 g nanopellets after reflux in pyridine.

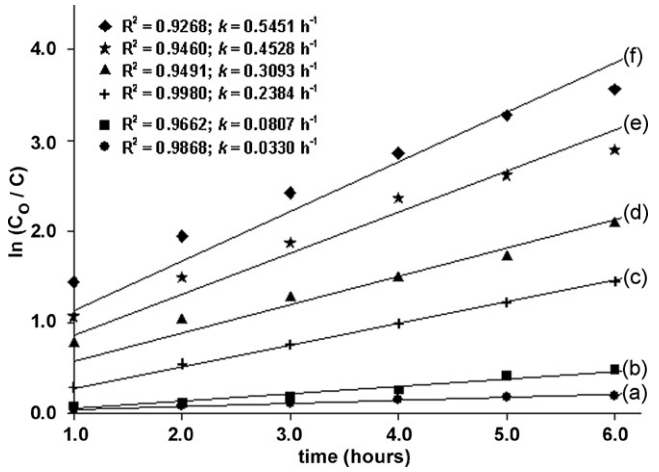

Fig. 4. Data re-plotted as $\ln(C_o/C)$ versus time which fitted to the pseudo-first-order-rate model for: (a) MB without catalyst, (b) 0.04 g 2D ZnO nanopellets before reflux in pyridine, (c) 0.001 g nanopellets after refluxed in pyridine, (d) 0.005 g nanopellets after reflux in pyridine, (e) 0.02 g nanopellets after refluxed in pyridine and (f) 0.04 g nanopellets after reflux in pyridine.

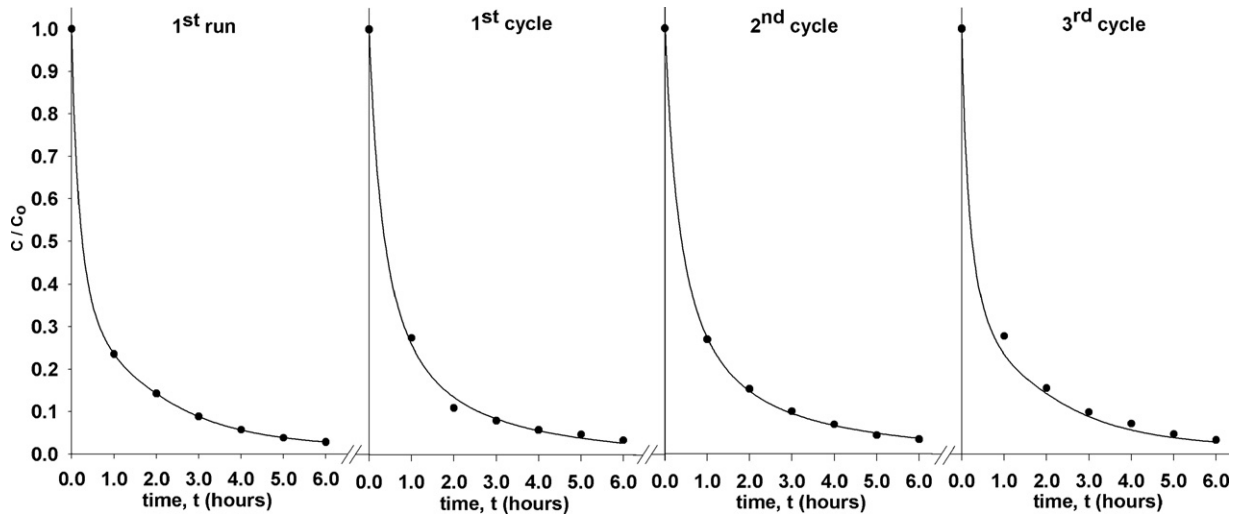

Fig. 5. Repeatability tests on photodecomposition of MB for three cycles by refluxed 2D ZnO nanopellets with the weight of 0.04 g.

0.0807 h^{-1} for the sample with 0.04 g 2D ZnO nanopellets (without being refluxed). By scrupulously refluxing the 2D ZnO nanopellets in pyridine, the *k* values were increased to 0.2384 and 0.3093 h^{-1}, respectively, for the nanopellets with the weight of 0.001 and 0.005 g. This could be attributed to the increasing surface area of nanopellets that would facilitate the absorption of MB. Furthermore, the removal of oleic acid also provides more reaction sites with higher electron densities for the absorption of MB and this greatly enhances the electron transfer rates between the nanopellets surfaces and MB molecules. These entire factors are highly beneficial in lowering the overall activation energy for the photodecomposition process to take place.

The *k* value for the sample with 0.02 g 2D ZnO nanopellets was determined to be 0.4528 h^{-1}. As a comparison, this value is higher than the *k* value reported by Wu et al. who deposited the own-synthesized titania nanoflower (0.0225 g) and commercialized Degussa P-25 nanoparticles (0.0225 g) on Ti substrate. They reported their *k* values to be 0.3540 h^{-1} for titania nanoflower film and 0.3360 h^{-1} for P-25 film [47]. The higher increase in rate constant of this sample in current study is technically better by applying the formation of free suspension, which renders higher surface area exposing to the light for electron transfer process, than that of fixed-bed photo reactor. Further increasing the weight of nanopellets to 0.04 g that is the maximum limit of photocatalytic dose in current study, the *k* value was calculated as 0.5451 h^{-1}. Subsequent weight increase in nanopellets to 0.05 g, the *k* value was decreased to 0.3938 h^{-1} (result not shown). The decrease of the rate constant could be attributed to the increase in turbidity that is caused by the exceeding amount of nanopellets used as the photocatalyst and this has reduced the light transmission through the solution. Thus, exceeding amount of photocatalyst may not be beneficial in view of possible interparticles aggregation as well as reduced irradiation field due to the increase in light scattering. In conjunction with this observation, Wei et al. who have conducted the photo-oxidation of phenol also reported that there is an optimum amount of TiO_2 loading as excessive amount of photocatalyst loading would have negative impact on the reaction rate [48].

However, the 2D ZnO nanopellets have lower photocatalytic rate if compared to that of commercialized ZnO nanoparticles. This could be due to the residual amount of oleic acid is still attaching on the surface of 2D ZnO nanopellets even though it has been refluxed for 8.0 h. The presence of this oleic acid is proven to hinder the absorption of MB on the photocatalyst surface. In addition, the variation in rate constants of these same materials could be caused by the differences in terms of morphology, primary and secondary particle size and specific surface area. In fact, this study has shown that the as-synthesized 2D ZnO nanopellets that have undergone refluxing process are exhibiting better photocatalytic ability in the photodecomposition of MB than that of without refluxed. Moreover, the unique nanofeature provided by 2D ZnO nanopellets is proven to assist in constraining the intermediates of MB and subsequently promote the further oxidation process as reported by Walker et al. [49]. In future, further treatment process will be carried out by coupling the UV–ozone (O_3) treatment on the as-refluxed 2D ZnO nanopellets since simultaneous action of ozone and ultraviolet can oxidize the oleic acid into carbon dioxide and water [35].

In order to elucidate the stability of the photoactivity for refluxed 2D ZnO nanopellets, cyclic experiments were carried out under the same experiment conditions. After the first run, the same nanopellets were reused for the subsequent cycle up to three cycles. According to the results (Fig. 5), only slight deactivation was observed after three cycles of photocatalytic tests. As a comparison between the repeatability test in first run and third cycle at sixth hour (Fig. 5), the amount of MB left in third cycle is slightly more than first run (0.43%). Hence, this implies that the as-synthesized 2D ZnO nanopellets are exhibiting excellent stability and recyclability.

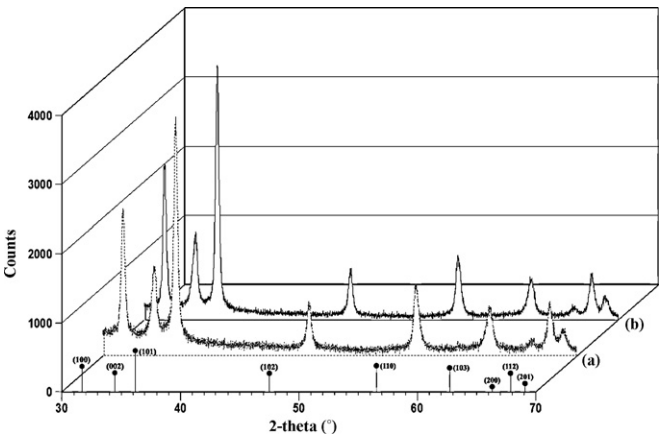

Fig. 6. XRD pattern of the refluxed 2D ZnO nanopellets (a) before photocatalytic test and (b) after three cycles of photocatalytic test on the photodecomposition of MB (● is the standard diffraction pattern).

Fig. 6 shows the XRD pattern of the refluxed 2D ZnO nanopellets before (Fig. 6(a)) and after (Fig. 6(b)) three cycles of photocatalytic test on the photodecomposition of MB. As shown in the XRD spectrums, there are no any significant changes even though after three cycles of photocatalytic test. All the peaks of both spectrums can be indexed to that of the standard ZnO with hexagonal wurtzite crystal structures (with space group *P*63*mc*) [50]. Additionally, no diffraction peaks from other impurities have been observed. This implies that the as-synthesized 2D ZnO nanopellets are highly stable and very suitable for photocatalytic applications, and it does not undergo any chemical changes if compared to other II–VI semiconductors [9–51].

4. Conclusion

In conclusion, the feasibility of own-synthesized 2D ZnO nanopellets in photodecomposition of MB has been tested. The surface chemistry was found to greatly influence its photocatalytic properties. Removal of the surface capping ligand through refluxing process has enhanced the photocatalytic efficiency of nanopellets. Furthermore, these nanopellets exhibit excellent recyclability up to three cycles. Thus, further developments and extension of current study for the photodegradation of various organic dyes in batch reactor are being pursued.

Acknowledgements

This project was supported by MOSTI under e-sciencefund (Project no.: 03-02-12-SF0019), techno-fund (Project no.: TF0106D212) and IRPA research grant (Project no.: 09-02-02-0032-SR0004/04-04). W.S. Chiu would like to thank Faculty of Engineering (University of Nottingham Malaysia Campus) for the research assistantship. The authors also would like to gratefully acknowledging Normalawati Bt. Shamsudin, Suhaniza Bt. Razali and Ahmad Zaki B. Zaini from the Electron Microscopy Unit (UKM) for their assistance in the TEM characterization. Finally, the authors would like to thank K.N. Wong (UKM) for fruitful discussions and technical advices.

References

[1] W.S. Chiu, P.S. Khiew, D. Isa, M. Cloke, S. Radiman, R. Abd-Shukor, M.H. Abdullah, N.M. Huang, Synthesis of two-dimensional ZnO nanopellets by pyrolysis of zinc oleate, Chem. Eng. J. 142 (3) (2008) 337–343.
[2] X. Wang, K. Maeda, A. Thomas, K. Takanabe, G. Xin, J.M. Carlsson, K. Domen, M. Antonietti, A metal-free polymeric photocatalyst for hydrogen production from water under visible light, Nat. Mater. 8 (1) (2009) 76–80.
[3] J. Tang, Z. Zou, J. Ye, Efficient photocatalytic decomposition of organic contaminants over $CaBi_2O_4$ under visible-light irradiation, Angew. Chem. Int. Ed. 43 (34) (2004) 4463–4466.
[4] P. Alivisatos, The use of nanocrystals in biological detection, Nat. Biotechnol. 22 (2004) 47–52.
[5] M. Bruchez, M. Moronne, P. Gin, S. Weiss, A.P. Alivisatos, Semiconductor nanocrystals as fluorescent biological labels, Science 281 (5385) (1998) 2013–2016.
[6] W.C.W. Chan, S.M. Nie, Quantum dot bioconjugates for ultrasensitive nonisotopic detection, Science 281 (5385) (1998) 2016–2018.
[7] V.L. Colvin, M.C. Schlamp, A.P. Alivisatos, Light-emitting diodes made from cadmium selenide nanocrystals and a semiconducting polymer, Nature 370 (6488) (1994) 354–357.
[8] W.U. Huynh, J.J. Dittmer, W.C. Libby, G.L. Whiting, A.P. Alivisatos, Controlling the morphology of nanocrystal-polymer composites for solar cells, Adv. Funct. Mater. 13 (1) (2003) 73–79.
[9] J.R. McBride, T.C. Kippeny, S.J. Pennycook, S.J. Rosenthal, Aberration-corrected *Z*-contrast scanning transmission electron microscopy of CdSe nanocrystals, Nanoletters 4 (7) (2004) 1279–1283.
[10] S. Funk, B. Hokkanen, U. Burghaus, A. Ghicov, P. Schmuki, Unexpected adsorption of oxygen on TiO_2 nanotube arrays: influence of crystal structure, Nanoletters 7 (4) (2007) 1091–1094.
[11] T. Zhang, T. Oyama, S. Horikoshi, J. Zhao, N. Serpone, H. Hidaka, Photocatalytic decomposition of the sodium dodecylbenzene sulfonate surfactant in aqueous titania suspensions exposed to highly concentrated solar radiation and effects of additives, Appl. Catal. B: Environ. 42 (1) (2003) 13–24.
[12] T. Zhang, L. You, Y. Zhang, Photocatalytic reduction of p-chloronitrobenzene on illuminated nano-titanium dioxide particles, Dyes Pigments 68 (2–3) (2006) 95–100.
[13] E.W. Kleefisch, Industrial Application of Titanium and Zirconium, ASTM International, USA, 1981.
[14] J. Emsley, Titanium. Nature's Building Blocks: An A–Z Guide to the Elements, Oxford University Press, Oxford, England, 2001.
[15] A. Sadao, II–VI Compound Semiconductors, Kluwer Academic Publishers, Massachusetts, USA, 2004.
[16] L. Kavan, M. Gratzel, S.E. Gilbert, C. Klemenz, H.J. Scheel, Electrochemical and photoelectrochemical investigation of single-crystal anatase, J. Am. Chem. Soc. 118 (28) (1996) 6716–6723.
[17] S. Sakthivel, B. Neppolian, M.V. Shankar, B. Arabindoo, M. Palanichamy, V. Murugesan, Solar photocatalytic degradation of azo dye: comparison of photocatalytic efficiency of ZnO and TiO_2, Sol. Energy Mater. Sol. C 77 (1) (2003) 65–82.
[18] J.H. Sun, S.Y. Dong, Y.K. Wang, S.P. Sun, Preparation and photocatalytic property of a novel dumbbell-shaped ZnO microcrystal photocatalyst, J. Hazard. Mater. 172 (2–3) (2009) 1520–1526.
[19] Z.L. Wang, Nanostructures of zinc oxide, Mater. Today 7 (6) (2004) 26–33.
[20] M.H. Huang, S. Mao, H. Feick, H. Yan, Y. Wu, H. Kind, E. Weber, R. Russo, P. Yang, Room-temperature ultraviolet nanowire nanolasers, Science 292 (5523) (2001) 1897–1899.
[21] M. Law, L.E. Greene, J.C. Johnson, R. Saykally, P. Yang, Nanowire dye-sensitized solar cells, Nat. Mater. 4 (6) (2005) 455–459.
[22] L.E. Greene, M. Law, D.H. Tan, M. Montano, J. Goldberger, G. Somorjai, P. Yang, General route to vertical ZnO nanowire arrays using textured ZnO seeds, Nanoletters 5 (7) (2005) 1231–1236.
[23] G. Shen, J.H. Cho, J.K. Yoo, G.C. Yi, C.J. Lee, Synthesis and optical properties of S-doped ZnO nanostructures: nanonails and nanowires, J. Phys. Chem. B 109 (12) (2005) 5491–5496.
[24] P.D. Yang, The chemistry and physics of semiconductor nanowires, Mater. Res. Bull. 30 (2) (2005) 85–91.
[25] E. Formo, E. Lee, D. Campbell, Y. Xia, Functionalization of electrospun TiO_2 nanofibers with Pt nanoparticles and nanowires for catalytic applications, Nanoletters 8 (2) (2008) 668–672.
[26] F. Zhao, X. Li, J.-G. Zheng, X. Yang, F. Zhao, K.S. Wong, J. Wang, W. Lin, M. Wu, Q. Su, ZnO pine-nanotree arrays grown from facile metal chemical corrosion and oxidation, Chem. Mater. 20 (4) (2008) 1197–1199.
[27] F. Li, Y. Ding, P.X.X. Gao, X.Q. Xin, Z.L. Wang, Single-crystal hexagonal disks and rings of ZnO: low-temperature, large-scale synthesis and growth mechanism, Angew. Chem. Int. Ed. 43 (39) (2004) 5238–5242.
[28] T.J. Kuo, C.N. Lin, C.L. Kuo, M.H. Huang, Growth of ultralong ZnO nanowires on silicon substrates by vapor transport and their use as recyclable photocatalysts, Chem. Mater. 19 (21) (2007) 5143–5147.
[29] M. Jose-Yacaman, C. Gutierrez-Wing, M. Miki, D.Q. Yang, K.N. Piyakis, E. Sacher, Surface diffusion and coalescence of mobile metal nanoparticles, J. Phys. Chem. B 109 (19) (2005) 9703–9711.
[30] K.J. Klabunde, J. Stark, O. Koper, C. Mohs, D.G. Park, S. Decker, Y. Jiang, I. Lagadic, D. Zhang, Nanocrystals as stoichiometric reagents with unique surface chemistry, J. Phys. Chem. 100 (30) (1996) 12142–12153.
[31] K.J. Klabunde (Ed.), Nanoscale Materials in Chemistry, John Wiley & Sons, Inc., USA, 2002.
[32] J. Tang, Z. Zou, J. Yin, J. Ye, Photocatalytic degradation of methylene blue on $CaIn_2O_4$ under visible light irradiation, Chem. Phys. Lett. 382 (1–2) (2003) 175–179.
[33] T. Zhang, T. Oyama, A. Aoshima, H. Hidaka, J. Zhao, N. Serpone, Photooxidative n-demethylation of methylene blue in aqueous TiO_2 dispersions under UV irradiation, J. Photochem. Photobiol. A: Chem. 140 (2) (2001) 163–172.
[34] W.S. Chiu, S. Radiman, M.H. Abdullah, P.S. Khiew, N.M. Huang, R. Abd-Shukor, One pot synthesis of monodisperse Fe_3O_4 nanocrystals by pyrolysis reaction of organometallic compound, Mater. Chem. Phys. 106 (2–3) (2007) 231–235.
[35] C. Aliaga, J.Y. Park, Y. Yamada, H.S. Lee, C.-K. Tsung, P. Yang, G.A. Somorjai, Sum frequency generation and catalytic reaction studies of the removal of organic capping agents from Pt nanoparticles by UV–ozone treatment, J. Phys. Chem. C 113 (15) (2009) 6150–6155.
[36] Y. Sui, X. Huang, Z. Ma, W. Li, F. Qiao, K. Chen, K. Chen, The effect of thermal annealing on crystallization in a-Si:H/SiO_2 multilayers by using layer by layer plasma oxidation, J. Phys.: Condens. Matter 15 (34) (2003) 5793–5799.
[37] M. Nakaya, M. Kanehara, M. Yamauchi, H. Kitagawa, T. Teranishi, Hydrogen-induced crystal structural transformation of FePt nanoparticles at low temperature, J. Phys. Chem. C 111 (20) (2007) 7231–7234.
[38] W.S. Chiu, S. Radiman, R. Abd-Shukor, M.H. Abdullah, P.S. Khiew, Tunable coercivity of $CoFe_2O_4$ nanoparticles via thermal annealing treatment, J. Alloys Compd. 459 (1–2) (2008) 291–297.
[39] J.R. Sachleben, E.W. Wooten, L. Emsley, A. Pines, V.L. Colvin, A.P. Alivisatos, NMR studies of the surface structure and dynamics of semiconductor nanocrystals, Chem. Phys. Lett. 198 (5) (1992) 431–436.
[40] J.E.B. Katari, V.L. Colvin, A.P. Alivisatos, X-ray photoelectron spectroscopy of CdSe nanocrystals with applications to studies of the nanocrystal surface, J. Phys. Chem. 98 (15) (2002) 4109.
[41] X.Y. Kong, Z.L. Wang, Spontaneous polarization-induced nanohelixes, nanosprings, and nanorings of piezoelectric nanobelts, Nanoletters 3 (2003) 1625–1631.

[42] J. Moser, S. Punchihewa, P.P. Infelta, M. Graetzel, Surface complexation of colloidal semiconductors strongly enhances interfacial electron-transfer rates, Langmuir 7 (12) (1991) 3012–3018.
[43] J.V. Stark, K.J. Klabunde, Nanoscale metal oxide particles/clusters as chemical reagents. Adsorption of hydrogen halides, nitric oxide, and sulfur trioxide on magnesium oxide nanocrystals and compared with microcrystals, Chem. Mater. 8 (8) (1996) 1913–1918.
[44] J.V. Stark, D.G. Park, I. Lagadic, K.J. Klabunde, Nanoscale metal oxide particles/clusters as chemical reagents. Unique surface chemistry on magnesium oxide as shown by enhanced adsorption of acid gases (sulfur dioxide and carbon dioxide) and pressure dependence, Chem. Mater. 8 (8) (1996) 1904–1912.
[45] R.W. Matthews, Photooxidation of organic impurities in water using thin films of titanium dioxide, J. Phys. Chem. 91 (12) (1987) 3328–3333.
[46] A. Mills, J. Wang, Photobleaching of methylene blue sensitised by TiO_2: an ambiguous system? J. Photochem. Photobiol. A: Chem. 127 (1–3) (1999) 123–134.
[47] J.-M. Wu, B. Huang, M. Wang, A. Osaka, Titania nanoflowers with high photocatalytic activity, J. Am. Ceram. Soc. 89 (8) (2006) 2660–2663.
[48] T.Y. Wei, C.C. Wan, Heterogeneous photocatalytic oxidation of phenol with titanium dioxide powders, Ind. Eng. Chem. Res. 30 (6) (2002) 1293–1300.
[49] S.A. Walker, P.A. Christensen, K.E. Shaw, G.M. Walker, Photoelectrochemical oxidation of aqueous phenol using titanium dioxide aerogel, J. Electroanal. Chem. 393 (1–2) (1995) 137–140.
[50] Joint Committee for Powder Diffraction Society (JCPDS), Powder Diffraction Database, pattern: 36-1451.
[51] N. Pinna, K. Weiss, H. Sack-Kongehl, W. Vogel, J. Urban, M.P. Pileni, Triangular CdS nanocrystals: synthesis, characterization, and stability, Langmuir 17 (26) (2001) 7982–7987.